JACS JOURNAL OF THE AMERICAN CHEMICAL SOCIETY

Article

Cite This: J. Am. Chem. Soc. 2018, 140, 3423−3433

pubs.acs.org/JACS

Catalytically Active Single-Chain Polymeric Nanoparticles: Exploring Their Functions in Complex Biological Media

Yiliu Liu,[#,†] Sílvia Pujals,[#,‡] Patrick J. M. Stals,[†] Thomas Paulöhrl,[†] Stanislav I. Presolski,[†] E. W. Meijer,[†] Lorenzo Albertazzi,[*,‡] and Anja R. A. Palmans[*,†]

[†]Laboratory for Macromolecular and Organic Chemistry and Institute for Complex Molecular Systems, Eindhoven University of Technology, P.O. Box 513, 5600 MB Eindhoven, The Netherlands

[‡]Institute for Bioengineering of Catalonia (IBEC), The Barcelona Institute of Science and Technology, Carrer de Baldiri Reixac 15-21, 08028 Barcelona, Spain

Supporting Information

ABSTRACT: Dynamic single-chain polymeric nanoparticles (SCPNs) are intriguing, bioinspired architectures that result from the collapse or folding of an individual polymer chain into a nanometer-sized particle. Here we present a detailed biophysical study on the behavior of dynamic SCPNs in living cells and an evaluation of their catalytic functionality in such a complex medium. We first developed a number of delivery strategies that allowed the selective localization of SCPNs in different cellular compartments. Live/dead tests showed that the SCPNs were not toxic to cells while spectral imaging revealed that SCPNs provide a structural shielding and reduced the influence from the outer biological media. The ability of SCPNs to act as catalysts in biological media was first assessed by investigating their potential for reactive oxygen species generation. With porphyrins covalently attached to the SCPNs, singlet oxygen was generated upon irradiation with light, inducing spatially controlled cell death. In addition, Cu(I)- and Pd(II)-based SCPNs were prepared and these catalysts were screened *in vitro* and studied in cellular environments for the carbamate cleavage reaction of rhodamine-based substrates. This is a model reaction for the uncaging of bioactive compounds such as cytotoxic drugs for catalysis-based cancer therapy. We observed that the rate of the deprotection depends on both the organometallic catalysts and the nature of the protective group. The rate reduces from *in vitro* to the biological environment, indicating a strong influence of biomolecules on catalyst performance. The Cu(I)-based SCPNs in combination with the dimethylpropargyloxycarbonyl protective group showed the best performances both *in vitro* and in biological environment, making this group promising in biomedical applications.

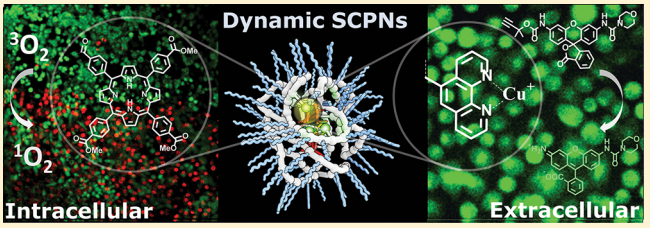

INTRODUCTION

Single-chain polymeric nanoparticles (SCPNs) are nanometer-sized objects obtained by controlling the global conformation of single polymer chains into well-defined, compartmentalized structures.[1] Nature represents a great source of inspiration for such architectures that aim to mimic the structural complexity as well as the functionality of the tertiary structure of proteins. A variety of synthetic approaches have been evaluated in order to obtain well-defined SCPNs.[2] The choice of the backbone, solubilizing pendant groups, and the functionalities responsible for the intrachain collapse or folding are all crucial for the development of effective SCPNs in a desired application. A key factor is the chemical moieties triggering the collapse/folding of the polymer backbone. In this framework two main approaches have been proposed: (i) the covalent (reversible or irreversible) cross-linking of chemical groups[3] and (ii) the use of reversible, supramolecularly interacting, pendant groups.[4] Notably, directional hydrogen-bond formation has been exploited to reversibly "lock" a flexible polymer into a specific conformation, which is often referred to as a "folding" process because of the reminiscence in which a polypeptide folds into α-helical and β-sheet structures. The intrinsic reversibility of hydrogen-bond interactions results in thermodynamically controlled formation of SCPNs, which are referred to as dynamic SCPNs because they can adapt to changes in the environment (temperature, pH, solvent). The choice of the folding strategy has a strong influence on the properties of the nanoparticles, e.g., on the particle stability and formation of multichain aggregates. A balanced choice of chemical structure and its folding processing steps are required to arrive at the required SCPN as pathway complexity very easily can give rise to instabilities and aggregation.[5]

In the past decade, SCPNs have been evaluated for a variety of applications in the field of catalysis,[6] material chemistry,[3h,7] imaging[8] and sensing.[9] Their small size (5−10 nm) and ease of functionalization are among the most attractive features that motivate the use of these polymeric architectures. These same features are attractive for the development of biomedical materials and systems, but biological applications of SCPNs are

Received: January 4, 2018
Published: February 19, 2018

DOI: 10.1021/jacs.8b00122
J. Am. Chem. Soc. 2018, 140, 3423−3433

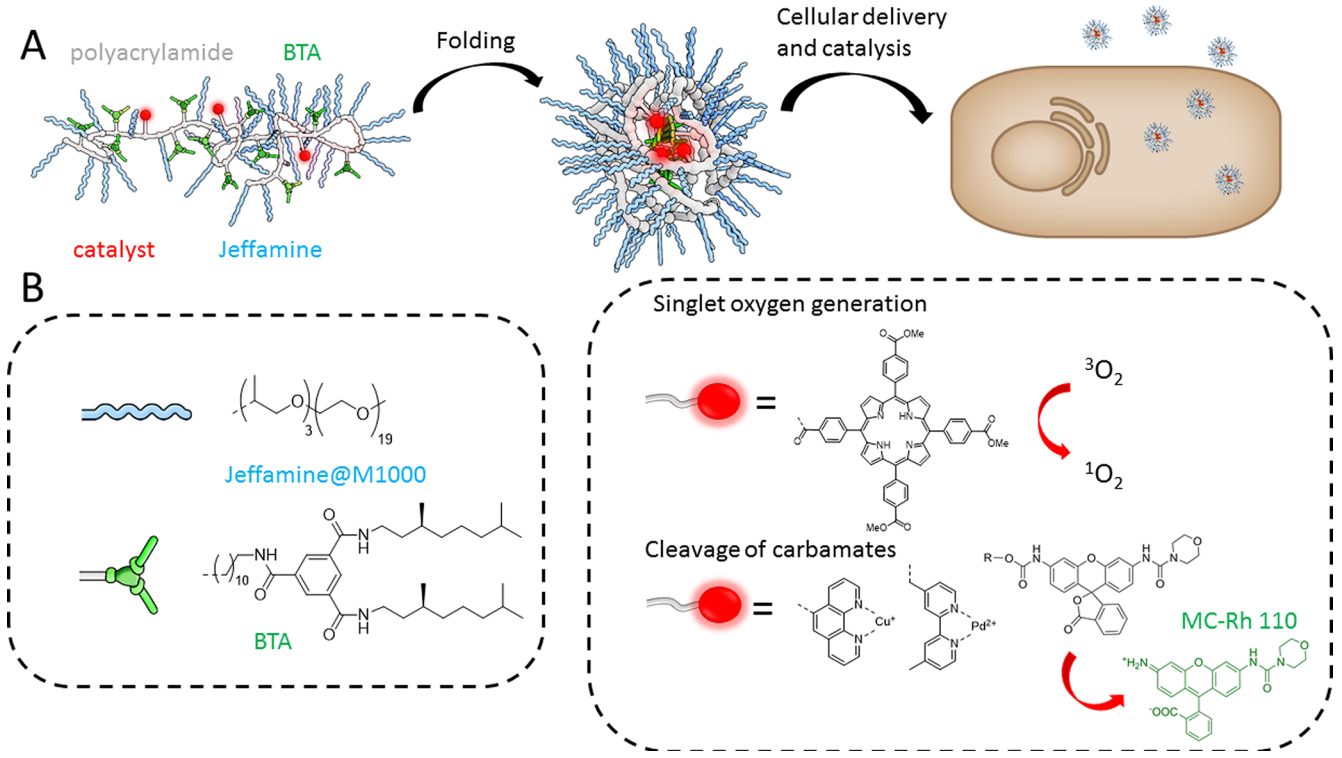

Figure 1. (A) General structure of the polymeric catalyst, its folding into a SCPN and its cellular delivery. (B) Chemical structures of the water-soluble side chains, the BTA-based folding motif, the catalysts and the substrates used in this study.

currently still scarce.[8b,10] One of the main reasons is a paucity in our knowledge on the behavior and stability of dynamic SCPNs in complex biological environments. This imposes challenges on the design of structures able to match the strict requirements of biological applications in terms of stability, toxicity, selective delivery, and performance.

In the past years, efforts in our group have been devoted to design dynamic SCPNs that are able to fold and perform a function, e.g., catalysis or sensing, in water.[6a,b,d,f,9] Recently, we introduced Pd-catalysts and singlet-oxygen generation porphyrins in water-soluble SCPNs and showed their folding and properties in aqueous media.[6f] In a next step, we became interested in evaluating how far SCPNs can affect the stability of the metal complex in cellular media and, at the same time, if the localization of the catalyst in the complex environment can be controlled. Here, we take this next step by performing catalysis in complex cellular environments using these nanoparticles. Performing bio-orthogonal chemistry and, more recently, bio-orthogonal catalysis inside living systems has attracted much attention.[11] Although the presence of amino acids, enzymes and glutathione poses challenges on the activity and stability of transition-metal based catalysts,[12] both the use of small transition-metal-based complexes[13] and metal-based nanoparticles/microspheres[14] have become promising approaches to convert artificial substrates inside living cells or in the extracellular environment. In particular, depropargylation reactions have been investigated as a way of *in vivo* deprotection of active moieties, e.g., prodrug activation.[15] Moreover, the synthesis of materials able to catalytically generate singlet oxygen is of great interest for applications in photodynamic therapy (PDT).[16]

Here we present a biophysical study of SCPN behavior in living cells and an evaluation of their performances in catalysis in complex biological environments. In our design (Figure 1), the SCPNs comprise a polyacrylamide-based backbone functionalized with (i) water-soluble side chains (oligo(ethylene oxide-*co*-propylene oxide) of DP = 22, Jeffamine@M-1000) to ensure water solubility; (ii) benzene-1,3,5-tricarboxamide (BTA) supramolecular moieties in order to trigger hydrogen-bonding-induced polymer folding and (iii) catalytically active sites. We first assess and optimize delivery strategies in order to target different compartments: the intracellular space, the cytoplasm or the endolysosomal compartment, and the extracellular space. This allows us to choose the delivery strategy depending on the desired applications. Next, we evaluate two activities to be performed in the cellular environment as shown in Scheme 1: (i) the photocatalytic generation of singlet oxygen ($^1O_2$) from molecular oxygen using A3B porphyrin moieties developed in our laboratory[17] and (ii) a catalytic cleavage of protective groups mediated by organometallic complexes based on Cu(I) and Pd(II). Both approaches give promising results, paving the way toward catalysis *in vivo* for biomedical applications. Moreover, our biophysical studies of SCPN behavior in living cells provides crucial information and will enable the rational design of improved nanosystems for catalysis-based therapies.

RESULTS AND DISCUSSION

Polymer Design. A small library of polymers varying in functionalization (Scheme 1) was designed and synthesized. A detailed description of the synthesis procedures and molecular characterization of the polymers is given in the Supporting Information (Schemes S1 and S2, Figures S1−S5). Typically, all polymers comprise around 10% BTA units and 80−90% water-soluble Jeffamine@M-1000, with degree of polymerization ranging from 120 to 150. **P1** and **P2** comprise 6% bipyridine or 8% phenantroline ligands to bind with Pd(II) and Cu(I), respectively. Phenantroline is well-known to bind Cu(II)

DOI: 10.1021/jacs.8b00122
J. Am. Chem. Soc. 2018, 140, 3423−3433

Scheme 1. Chemical Structures of the Polymers P1−P4 Applied in This Work[a]

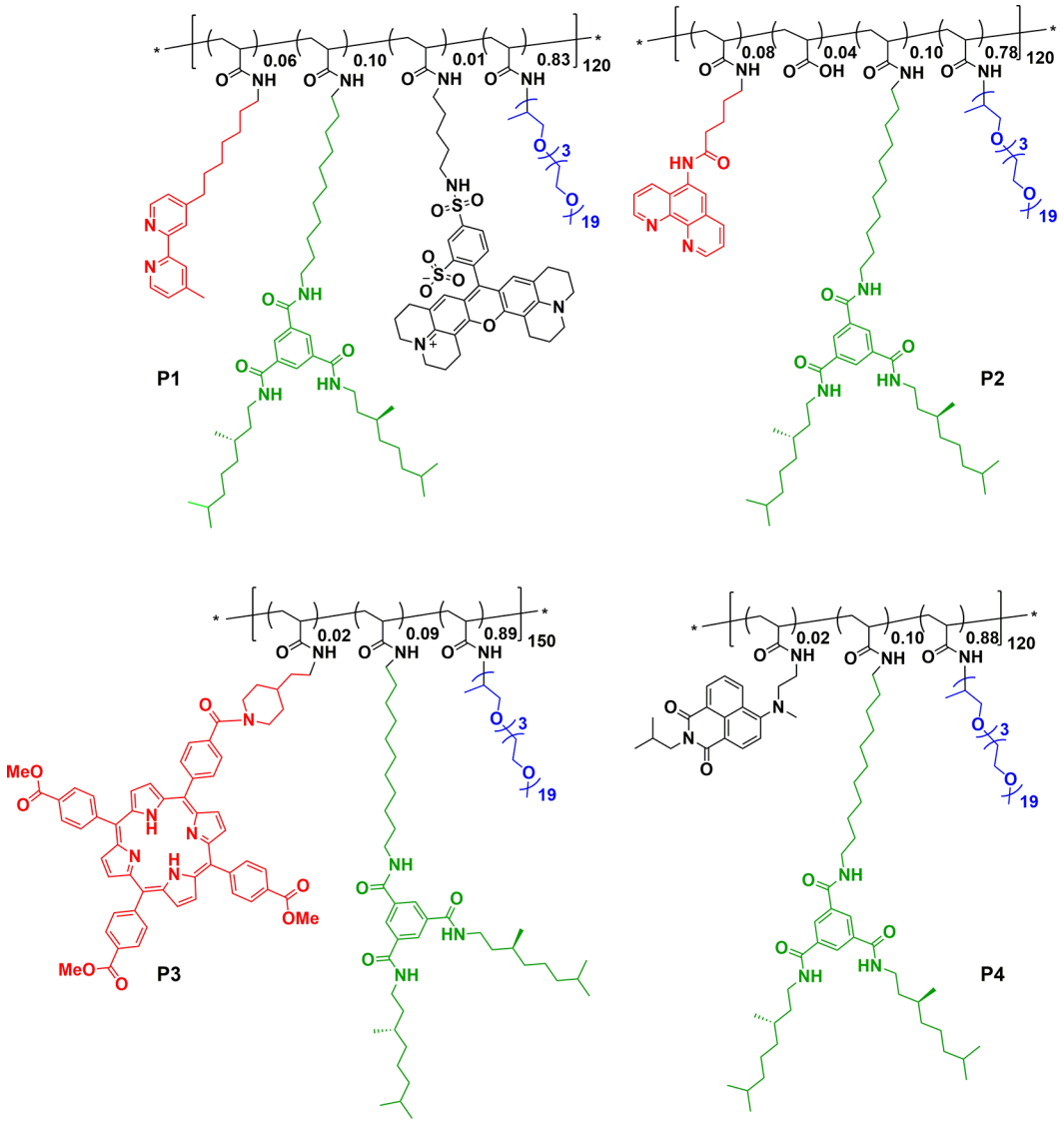

[a]**P1** comprises a 2,2′-bipyridine ligand and Texas Red dye, **P2** comprises a phenanthroline ligand, **P3** a porphyrin and **P4** a naphthalimide-based fluorophore.

and accelerate azide−alkyne cycloaddition reactions upon reduction of Cu(II) to Cu(I) *in situ*.[18] In addition, bipyridine complexes with Pd(II) have been studied extensively and were found to be active in a variety of catalytic reactions.[19]

The binding of Pd(II) to the bipyridine ligands in **P1** and binding of Cu(II) to the phenantroline ligands in **P2** were checked by UV−vis spectroscopy. Upon addition of metal ions, clear red shifts in the absorption of the ligands were observed, suggesting the formation of the organometallic complex (Figure S2). The effect of the presence of metals on polymer chain folding via BTA aggregation was evaluated by circular dichroism spectroscopy. The Cotton effects were not significantly affected by the presence of the metal indicating that metal complexation does not interfere with BTA aggregation in these systems (Figures S3 and S4). This is in line with previous observations in similar polymers.[6d,f] In addition, the predominantly single chain character of the formed particles before and after metal complexation was verified by dynamic light scattering, respectively (Figure S5).

We previously showed that polymer **P3**, which comprises 2% of porphyrin moieties, is active in photosensitization.[6f] The formation of SCPNs in aqueous solution was shown to isolate the porphyrin moieties, preventing undesired porphyrin aggregation. Hereby, the photocatalytic efficiency in singlet oxygen generation was promoted. Polymers with covalently attached fluorescent dyes (1% Texas Red in **P1** and 2% naphthalimide-based fluorophore in **P4**, Scheme 1) were prepared, to allow their visualization with confocal microscopy. In the case of **P4**, the solvatochromic character of the naphthalimide-based fluorophore is useful to obtain information on the polarity of the environment.[20]

Delivery Strategies for SCPNs. Three delivery strategies shown in Figure 2 were evaluated to selectively localize SCPNs based on **P1** (without metals) in the desired cellular compartment by tracking the emission of Texas Red. First, administration of SCPNs in the medium at high concentration (2.5 mg mL^{-1}) was used to deliver SCPNs into HeLa cells via an endocytic route. Although the oligo(ethylene oxide)-based pendants of the polymers reduce the interactions with cells,

DOI: 10.1021/jacs.8b00122
J. Am. Chem. Soc. 2018, 140, 3423−3433

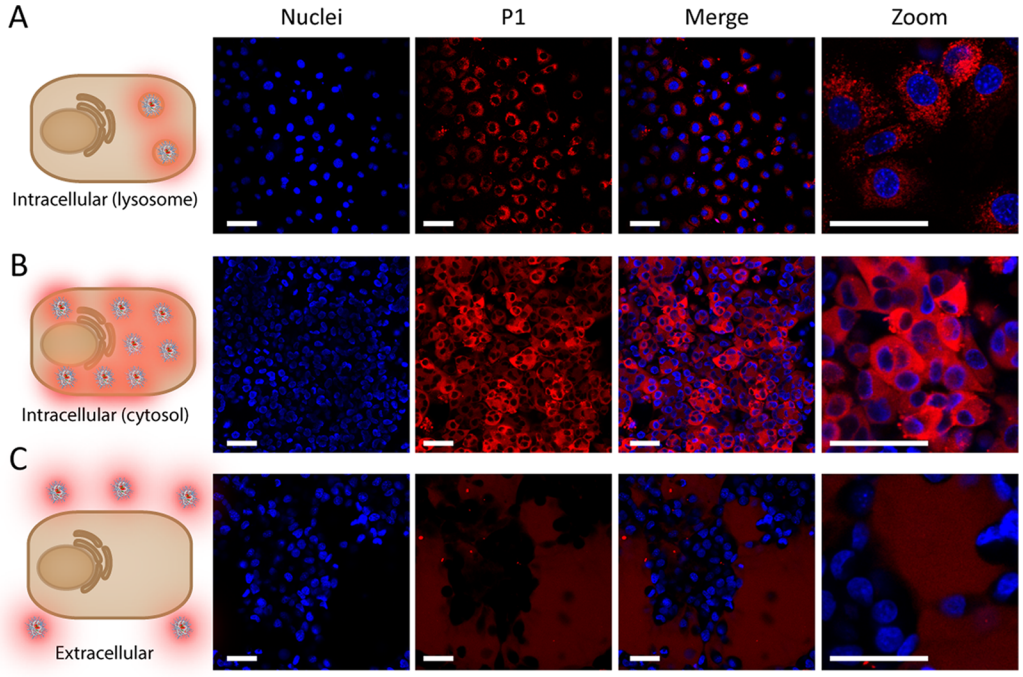

Figure 2. Confocal imaging of HeLa cells using different approaches for **P1**-based SCPN delivery. The red color indicates Texas Red fluorescence of the SCPNs whereas the blue color arises from cell nuclei stained with Hoechst. (A) Cell internalization by administration into the medium at high concentration (2.5 mg mL^{-1}) for 24 h via endocytosis and consequent lysosomal localization of **P1**. (B) Intracellular delivery via electroporation and consequent cytosolic localization of **P1**. (C) Extracellular localization by administration of **P1** to the medium at 1.0 mg mL^{-1} for 3 h. Scale bar = 50 μm.

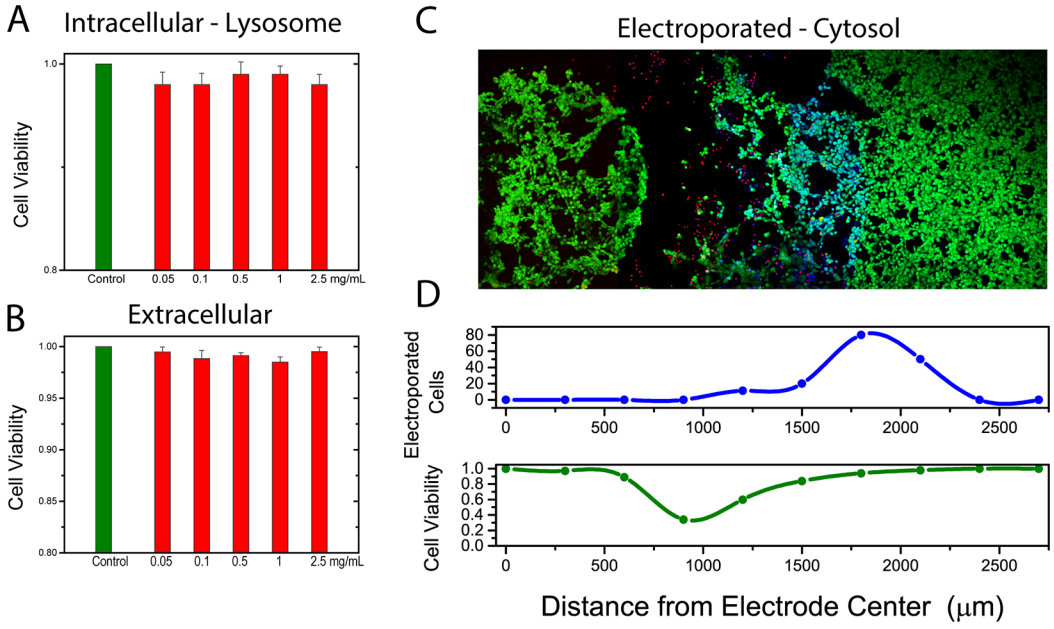

Figure 3. Toxicity of **P1** measured with live/dead assays. (A,B) Cell viability of HeLa cells at after SCPN internalization different **P1** concentration (red bars) (A) and extracellular treatment (B), the viability of untreated cells is added as a control (green bars). (C) Imaging of the zone of electroporation. Green = live cells, red = dead cells, blue = electroporated cells. (D) Spatial distribution of cell viability depending on the distance from the electrodes. Notably, there is a decrease in cell viability only due to the mechanical pressure of the electrodes while the electroporated cells that take up **P1** do not show any toxicity.

accumulation of SCPNs was observed slowly over time, displaying the characteristic vesicular localization of the endolysosomal system (see Figure 2A). This behavior was also observed when working with other cell lines as shown in Figure S6. The slow internalization is not surprising; many reports describe cell internalization of PEGylated particles of similar size, which eventually accumulate in the lysosome.[21] To confirm the lysosomal localization, a colocalization assay with lysosome markers was performed. Figure S7 shows a high degree of colocalization of SCPNs with lysosensor after 24 h,

DOI: 10.1021/jacs.8b00122
J. Am. Chem. Soc. 2018, 140, 3423−3433

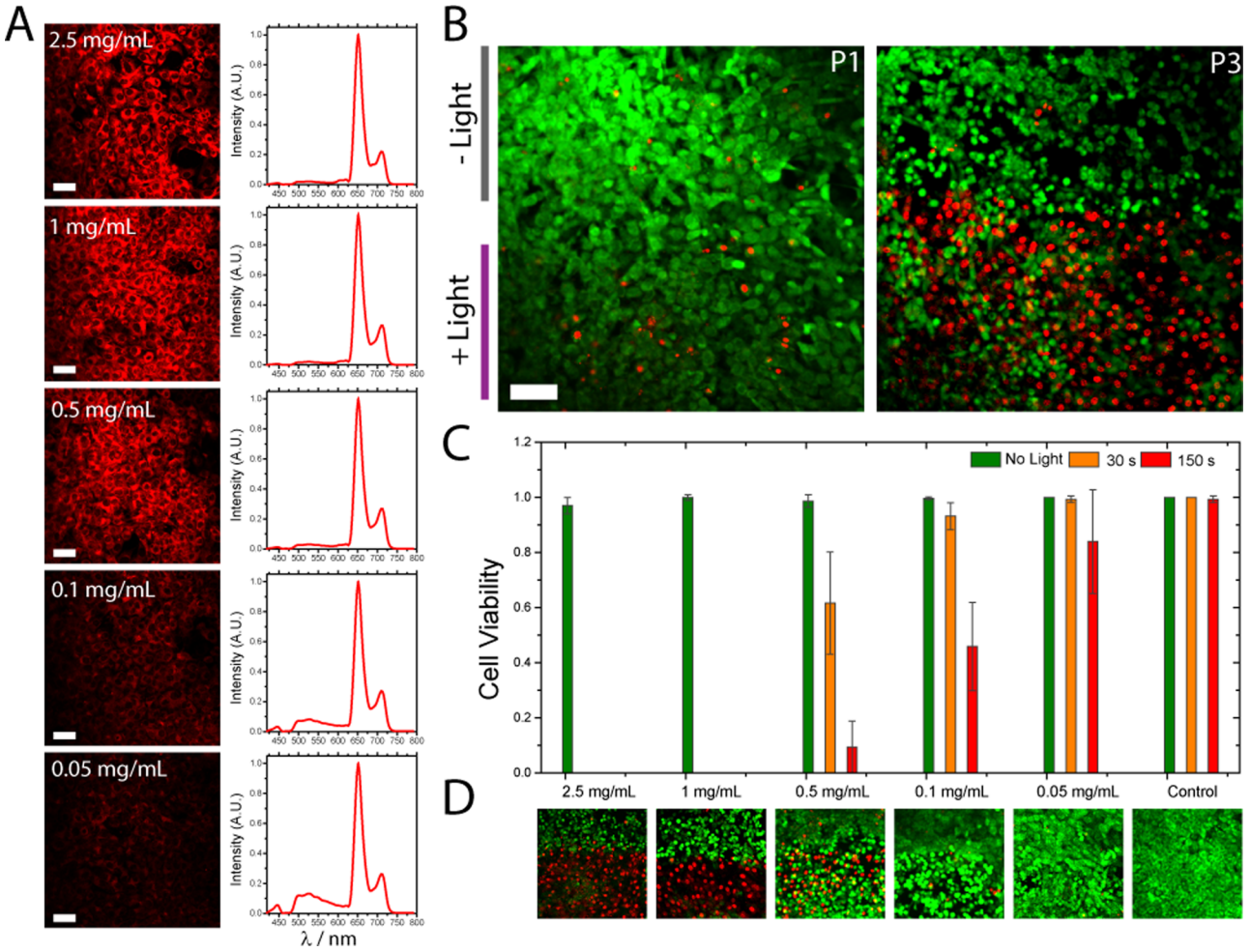

Figure 4. Photogeneration of singlet oxygen in HeLa cells incubated with different concentrations of **P3**-based SCPNs for 24 h. (A) Confocal imaging of HeLa cells treated with different concentrations of **P3** showing a concentration-dependent uptake. (B) Confocal imaging of a live/dead assay on HeLa cells treated with **P1** (left) and **P3** (right). The field of view shows an area irradiated with UV light (λ = 403 nm) for 150 s. (C) Quantification of cell viability at different polymer concentrations and UV irradiation times of 30 and 150 s. (D) Corresponding confocal live/dead assay of the different polymer concentrations (30 s irradiation). Scale bar = 50 μm. The UV irradiation was performed with a 403 nm laser, which has average power of 160 mW per pulse (55 ps per pulse), at a repetition rate of 42 MHz.

confirming our hypothesis. Lysosomal localization has been observed for a variety of nanoparticles used for drug delivery and the low pH of this organelle can be exploited by pH-responsive materials.[22]

Although lysosomal localization could be interesting in the context of delivery, the SCPNs cannot reach most of the cellular structure. Therefore, we followed a second delivery strategy based on electroporation. Electroporation, the temporary permeabilization of a cell membrane with electric pulses, is a standard technique for the cytosolic delivery of biological macromolecules, e.g., DNA for transfection,[23] and its use for synthetic polymers and particles has recently been reported.[22b,24] Here we apply this technique to deliver SCPNs based on **P1** into the cytosol of HeLa cells. Figure 2B shows the localization of SCPNs following electroporation. The SCPNs are homogeneously distributed inside the cytoplasm but excluded entirely from the nucleus. This finding is similar to what has been reported for dendrimers and recombinant proteins, and not surprising taking the size of SCPNs into account, which exceeds the size of the nuclear pore.[25] The perfectly homogeneous distribution inside the cytosol is a good indication that the oligo(ethylene oxide)-based chains are able to shield the hydrophobic core effectively, preventing interactions with cellular membranes and improving SCPN stability in the cellular media.

Last, we investigate the possibility to use SCPNs in the extracellular space. This is of interest for a variety of pharmaceutical applications where drug release from prodrug activation should happen at the tissue level, i.e., outside cells. Figure 2C shows the extracellular localization of **P1**-based SCPNs administered in the medium. Due to the shielding of the oligo(ethylene oxide)-based chains, the interactions with cell membrane are minimized and the SCPNs mostly localize in the extracellular space for several hours at the concentration (1 mg mL^{-1}) used. The balance between endocytic internalization and permanence in the extracellular space can thus be tuned by polymer concentration and internalization time. Importantly, this behavior is not affected if the SCPNs are complexed with the metal, as shown in Figure S8. If desired, the SCPNs can be functionalized with cell penetrating peptides or with surface charge. This will promote cell internalization.[26a,b] In contrast, a more effective shielding will expand the lifetime in the extracellular space.[26c,d]

DOI: 10.1021/jacs.8b00122
J. Am. Chem. Soc. 2018, 140, 3423−3433

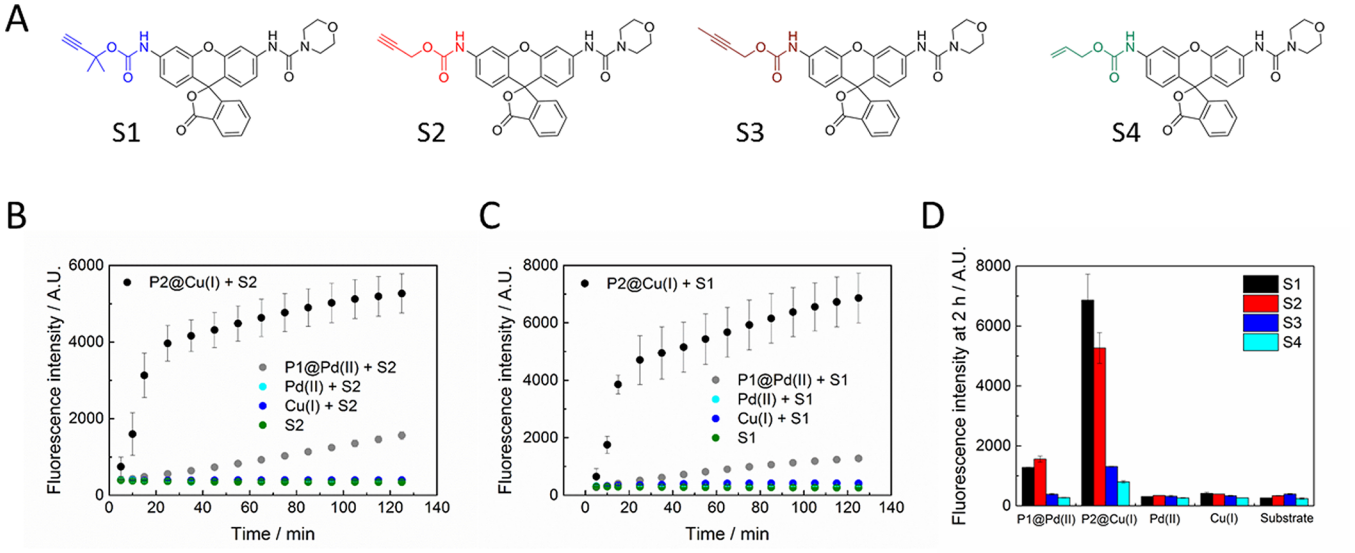

Figure 5. Results for the deprotection reactions of protected rhodamines by SCPN-based catalysts in the presence of HeLa cells. (A) Chemical structures of the substrates **S1**−**S4** used in this study. (B,C) Kinetic profile of the deprotection reaction of **S2** (B) and **S1** (C) with SCPNs based on **P2@Cu(I)** and **P1@Pd(II)** followed for 2 h in the presence of cell medium and HeLa cells. As a control, the activity of "free" metal catalysts (Cu(I) and Pd(II)) and no catalyst in the deprotection of **S1** and **S2** are added. (Reaction conditions: concentration of substrate (**S1**/**S2**) = 30 μM; **P1@Pd(II)**: [Bipy] = 60 μM; [Na_2PdCl_4] = 50 μM; **P2@Cu(I)**: [Phen] = 66.7 μM; [$CuSO_4$] = 33.3 μM, (phen:Cu = 2:1), [NaAsc] = 1 mM). The conversion was monitored by fluorescence detection of the product MC-Rh 110 at different time intervals. (D) Histogram summarizing the fluorescence intensity of MC-Rh 110 after 2 h of reaction for different catalysts, substrates and controls.

Biocompatibility and Folding State of SCPNs. Having developed reliable procedures for selective cell delivery, we evaluated the biocompatibility of the SCPNs in the three compartments studied. A live/dead assay using calcein AM/propidium iodide was performed to assess the toxicity after cytosol, lysosome and extracellular space delivery.[27] Figure 3A,B shows the cell viability of untreated cells (green bars) and cells after administration of **P1**-based SCPNs in the lysosome and extracellular space at different concentrations (red bars). No significant changes in cell viability were observed when **P1** was delivered via endocytosis or incubated for 3 h in the extracellular space. This indicates that the SCPN architectures are not toxic, most probably due to the oligo(ethylene oxide)-based layer preventing harmful cell−material interactions.

The cytosolic delivery deserves a separate discussion. The electroporation procedure is intrinsically harmful for cells and the toxicity due to the delivery procedure should be disentangled from the possible toxicity due to the SCPNs. Figure 3C shows confocal imaging of cells electroporated with **P1**-based SCPNs and treated with the live/dead reagent: green cells are viable cells, red cells are nonviable and the SCPN signal is reported in blue. The image clearly shows a noticeable layer of dead cells. This layer coincides with the donut-shaped electrode that "smashed" those cells during the electroporation procedure. In contrast, cells that were not mechanically perturbed by the electrode are viable. It is now important to assess if the **P1**-containing cells are viable as well. Figure 3D reports the cell viability and the SCPN signal as a function of the distance from the electrode. As can be seen from the plot in Figure 3D there is significant cell death associated with the mechanical stress of the electrode, but no significant toxicity is observed among the electroporated cells. This indicates that the use of SCPNs does not result in alteration of cell viability when delivered into the cytosol.

The folding in the dynamic SCPNs applied here, relies on reversible intramolecular hydrogen-bond formation in combination with a hydrophobically driven collapse.[5] Hence, it is important to assess whether SCPNs undergo large conformational changes when they are in contact with the cellular media. For this purpose, **P4** decorated with a solvatochromic naphthalimide-based fluorophore was employed. As shown in Figure S9, the emission wavelength of **P4** undergoes clear shifts in solvents of varying polarity. Noteworthy, **P4** shows an emission peak at 527 nm in water while the free naphthalimide dye (Naph-Amine, Figure S10) has an emission at around 540 nm; such a difference in the wavelength of emission confirms that the SCPNs provide a less polar interior. **P4** and the free naphthalimide dye were then tested in the presence of serum containing cell medium. Though the free naphthalimide dye is highly sensitive to the cellular environment, this is much less the case for **P4** (see Table S1). This suggests that the SCPNs provide a structural shielding and reduce the effects from the outer environment, e.g., serum proteins. Although this does not conclusively show that **P4** remains in a folded conformation, i.e., intact hydrogen bonds between the BTA units, it does show that the cellular medium does not significantly alter the environment of the fluorophore, indicating that the SCPNs still provide a rather stable, hydrophobic environment.

Singlet Oxygen Generation with SCPNs. The above results show that SCPNs are stable and nontoxic for cells. Our next step is to deliver and test the performances of functional SCPNs. We first focus on **P3**, which comprises porphyrin units that can generate singlet oxygen upon irradiation with light.[6f] The use of SCPNs to prevent porphyrin aggregation may pose advantages compared to previously applied approaches (such as dendrimers or polymer micelles)[28] because they combine easy accessibility with high stability. Figure 4A shows the delivery of SCPNs based on **P3** via endocytosis at different concentrations. A good correlation of the amount internalized with the concentration of incubation was observed. Furthermore, the emission spectra of the porphyrin (Figure 4A, right) are not

DOI: 10.1021/jacs.8b00122
J. Am. Chem. Soc. 2018, 140, 3423−3433

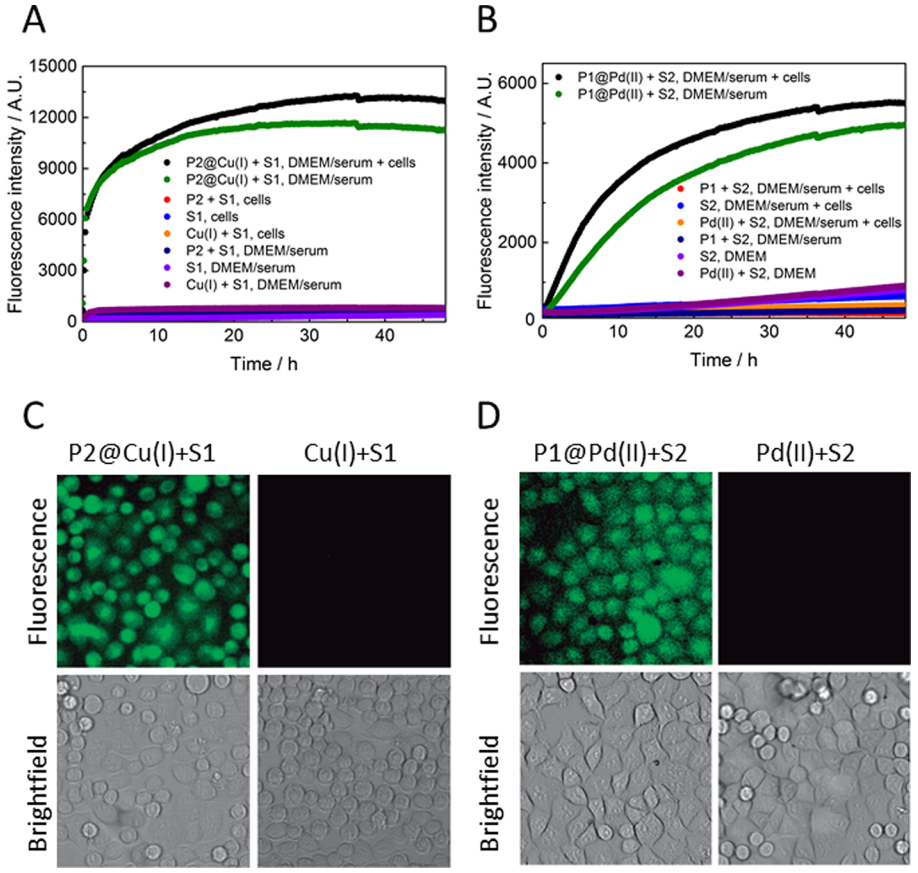

Figure 6. Kinetics of the deprotection reactions followed for 48 h using SCPNs in complex media. **P2@Cu(I)** catalyzed depropargylation reaction of **S1** (A) and **P1@Pd(II)** of **S2** (B) with or without HeLa cells in full cellular medium (DMEM + 10% serum). (**P1@Pd(II)**: [Bipy] = 60 μM; [Na_2PdCl_4] = 50 μM, [**S2**] = 30 μM; **P2@Cu(I)**: [Phen] = 66.7 μM; [$CuSO_4$] = 33.3 μM, [**S1**] = 30 μM, [NaAsc] = 1 mM). Catalysis was monitored by fluorescence detection of MC-Rh 110 at different times. (C,D) Imaging of HeLa cells incubated with the substrates together with SCPNs complexed with the metals or with the metals alone. Upper panels: fluorescence emission at 488 nm (FITC filter); lower panels: bright field.

affected by cell internalization at any concentration studied, indicating minimal perturbation of the functional unit.

Figure 4B reports a live/dead test assessing the toxicity in the dark as well as the phototoxicity after 403 nm irradiation of SCPNs based on **P3** compared with a control performed by a Texas red functionalized SCPN of **P1**. A minimal toxicity was observed for the nonactive SCPN (**P1**) that can be associated with the UV exposure alone. On the contrary, the porphyrin-based SCPN (**P3**) induces significant cell death after irradiation, which is in agreement with its ability to generate singlet oxygen. We further investigated the performance of **P3** to induce light-mediated cell death. Figure 4C shows the cell viability in the irradiated area at different concentrations of the particle and different light doses. Up to 0.05 mg mL^{-1} no cell death is observed after irradiation at all light dose. On the contrary at 0.1 and 0.5 mg mL^{-1}, the intracellular concentration of SCPNs is sufficient to induce toxicity in a light-dependent manner. At 1 and 2.5 mg mL^{-1}, complete cell death was observed at all light dose studied. This is further corroborated by the live/dead assay in Figure 4D, which shows an analogous trend. These measurements indicate that SCPNs internalized in cells generate singlet oxygen which induces cell death. Therefore, SCPNs are effective carriers of single-oxygen generators, paving the way toward their use as PDT agents.

Catalysis in Complex Media with SCPNs. Finally, we investigated the ability of metal-loaded SCPNs to catalyze chemical reactions in biological media. **P1** and **P2** contain bipyridine or phenanthroline ligands that can bind to Pd(II) or Cu(I) ions to form organometallic catalytically active sites. In all catalysis experiments, we applied the complex formed by **P1** and Na_2PdCl_4 directly, whereas the complex formed by **P2** and $CuSO_4$ was reduced in situ by sodium ascorbate (NaAsc). The catalysis experiments were performed with low concentrations of **P1** and **P2** (1 mg mL^{-1}) and short incubation times to limit uptake of the polymers by endocytosis. This favors catalysis occurring in the extracellular environment. We focus on metal-catalyzed carbamate cleavage reactions[29] to evaluate these SCPN-based catalysts inspired by the reported bio-orthogonality of these reactions[13a,c,14c,d] and the possibility to design catalyst-triggered anticancer drugs based on these protective groups.[15] A series of fluorogenic substrates **S1**-**S4** were designed and synthesized as shown in Figure 5A, which all comprise one carbamate protected amine.[13a,b,15a] **S1**-**S4** are nonemissive molecules, however, cleavage of the carbamate-based protection group results in the highly fluorescent product-molecule morpholinecarbonyl rhodamine 110 (MC-Rh 110).[30] Apart from the previously used propargyloxycarbonyl (**S2**) and allyloxycarbonyl (**S4**) groups, we also include the dimethylpropargyloxycarbonyl group (**S1**), which was recently predicted to have potential in bio-orthogonal cleavage reactions as it hydrolyzed in the presence of Cu(I) instead of undergoing a "click" reaction with azides.[11h,31] We also include a protective group comprising an inner alkyne (**S3**).

DOI: 10.1021/jacs.8b00122
J. Am. Chem. Soc. 2018, 140, 3423−3433

An *in vitro* study showed that **P1@Pd(II)** and **P2@Cu(I)** are effective catalysts in deprotecting **S1** and **S2** (Figures S11 and S12), with the deprotection of **S1** catalyzed by **P2@Cu(I)** showing the fastest rate. In addition, the SCPN-based catalysts showed much higher turnovers than the corresponding small molecule metal–ligand complexes BiPy@Pd(II) and Phen@Cu(I).[32] In fact, we found that the local medium effect of SCPNs, such as accumulation of hydrophobic substrates and catalytically active sites, significantly promotes their catalytic performance.[32] On the basis of the *in vitro* study, we here focus on **P1@Pd(II)** and **P2@Cu(I)** for further evaluation in cellular environments.

Before performing the catalysis experiments in cells, we assessed that the SCPNs complexed with the metals do not exert toxicity to the HeLa cells. The SCPNs were complexed with their respective metals (**P1@Pd(II)** and **P2@Cu(I)**) and incubated in full medium with cells for 4 and 24 h. As can be seen in Figure S13, evaluation of viability of HeLa cells using the Presto Blue assay shows that the catalytic system **P1@Pd(II)** and **P2@Cu(I)** does not show cytotoxicity, also not when only the metals salts are applied. The toxicity was also evaluated in the presence of the different substrates, which showed that there was no negative effect of the whole catalyst/substrate system on the cells.

Having established that metal-based SCPNs are not toxic for HeLa cells, we proceeded with catalysis studies. HeLa cells were incubated with the catalysts (**P1@Pd(II)** or **P2@Cu(I)**) and one of the **S1**–**4** substrates for 2 h in the presence of the cell medium (DMEM supplemented with serum); the results are shown in Figure 5B,C (**S1**, **S2**) and Figure S14 (**S3**, **S4**). Figure 5B,C shows that both catalysts are able to convert **S1** and **S2** into the fluorescent product MC-Rh 110 while all the controls tested (only metal salt as the catalyst, no catalyst) do not show a significant activity. A number of interesting observations can be made. First, when applying the copper-based catalyst **P2@Cu(I)** the fluorescence intensity increases much faster and to a higher level for both **S1** and **S2** than when using the palladium-based **P1@Pd(II)**. The deprotection of the dimethylpropargyloxycarbonyl group in **S1** is known to occur fast in the presence of Cu(I),[31b,32] in aqueous solutions but has not been investigated in complex biological media. Second, **S3** and **S4** (Figures S14) show a limited conversion with **P2@Cu(I)** and no conversion for **P1@Pd(II)**. Most likely, the terminal alkene in **S4** and methyl acetylene group in **S3** cannot bind as effectively to Cu(I)/Pd(II) as a result of the deprotection mechanism. This is postulated to occur via a terminal alkyne, which is the case of **S3** is not feasible.[13e,31b] Interestingly the catalysts also have different preferences for substrates: **P2@Cu(I)** performs best with **S1** while **P1@Pd(II)** has a slight preference for **S2**. Therefore, a clear trend (**S1** > **S2** ≫ **S3** > **S4**) is present for copper and **S2** > **S1** ≫ **S3** = **S4** for palladium, as highlighted by the histogram in Figure 5D. The results clearly show that the deprotection reaction using SCPNs is feasible in such complex biological media, albeit less efficient than when the deprotection is performed in PBS only (Figure S15).

For the two best performing catalyst/substrate pairs, we repeated the kinetic measurements for a longer time (up to 60 h) in cells with DMEM medium or in DMEM medium only. Figure 6 shows the results of the development of the fluorescence over 48 h for **P2@Cu(I)** with **S1** (Figure 6A) and **P1@Pd(II)** with **S2** (Figure 6B). Both catalysts perform very well compared to all the controls tested and show a significant increase in fluorescence intensity, which reaches a plateau in about 24 h for copper and 48 h for palladium. The findings are further supported by fluorescence microscopy that allows to visualize the conversion of the substrates into MC-Rh 110. The formed MC-Rh 110 diffuses through the cell membranes and thus shows fluorescence inside the cells (Figure 6C,D). Although the differences in mitochondrial activity are small (Figure S13), the cell morphology changed when using Cu(I) as the catalyst compared to Pd(II), indicating an onset of toxicity when using Cu-based catalysts. Interestingly, no appreciable difference is found between the sample containing cells and the one with medium only, indicating that the presence of the cells does not affect catalytic performance.

The investigations presented here are primarily aimed at achieving a rational understanding of the catalyst behavior and activity in the presence of biological molecules. The results shown above clearly indicate that Pd(II)- and Cu(I)-based SCPNs are capable of deprotecting **S1** and **S2** into MC-Rh 110 in the presence of cells. We also identified the complexities involved. Figure 7 summarizes the effect of medium and

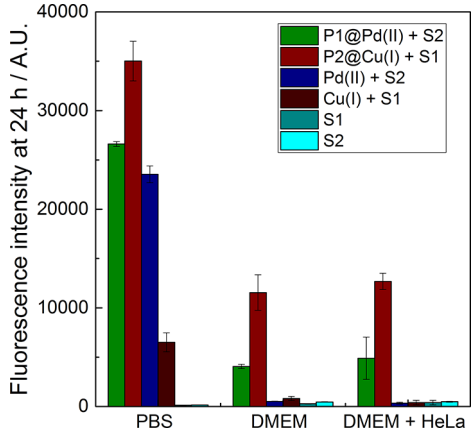

Figure 7. Comparison of the fluorescence intensity reached after 24 h of reaction under different conditions, including Cu(I) and Pd(II) based catalysts with or without SCPNs and reference experiments in different media. In all cases, DMEM was supplemented with 10% serum.

medium with cells on the activity of SCPNs in the depropargylation of **S1** and **S2** compared to the activity in PBS buffer. The plateau of the fluorescence intensity that is reached after 24 h in the presence of medium is at a lower level than when performing the catalysis in PBS. This suggests that the performance of the SCPN-based catalysts is negatively affected by the presence of serum proteins present in the DMEM medium. Interestingly, the additional presence of cells has no further negative effect on the fluorescence intensity reached after 24 h. This can be rationalized by two factors (or a combination of the two): (i) the sequestration of hydrophobic substrates by serum protein binding and (ii) the serum proteins inactivate the catalyst. The fact that the catalyst in DMEM reaches a plateau before full conversion is reached, seems to indicate that the catalyst loses efficacy over time. Although little has been reported to date on the long-term stability of small transition-metal-based catalysts in serum or cellular media, it is likely that in previously reported examples, the metals also become sequestered by reactive groups present on the protein surfaces over time. In addition, Figure 7 shows that the metal-catalyzed deprotection reaction of both propargyl-protected

DOI: 10.1021/jacs.8b00122
J. Am. Chem. Soc. 2018, 140, 3423–3433

substrates in the absence of the SCPNs is more prominent in PBS buffer than in DMEM with or without HeLa cells. This indicates that the activity of the catalyst inside the SCPN is significantly enhanced in cellular media compared to that of the metal salt. Finally, hydrolysis of the substrates in the absence of any catalyst is more significant in the biological environment than in PBS. Nonmetal-catalyzed hydrolysis can become an issue at longer time scales in biological media.

CONCLUSIONS

In this work, we show the results of a biophysical study of dynamic single-chain catalytic polymeric nanoparticle activity in a biological environment. Several administration strategies were successfully developed, allowing the delivery of SCPNs in the extracellular space, in the endolysosomal compartment, and in the cytosol. The SCPNs, even those comprising transition-metal-based catalysts, showed excellent biocompatibility and did not show significant toxicity toward cells. In addition, evidence is presented that the dynamic SCPNs create a rather stable environment for the catalytic species.

Two strategies to assess the viability of the use of SCPNs in complex biological media were investigated. Irradiation with light successfully generated singlet oxygen and promoted light-induced localized toxicity when porphyrin-based SCPNs were introduced via endocytosis into cells. This makes these SCPNs highly interesting for future applications in photodynamic therapy. In addition, Pd(II) and Cu(I) loaded metal-based SCPNs showed an efficient depropargylation of protected rhodamine in the extracellular space. Notably, Cu(I)-based SCPNs in combination with a dimethylpropargyloxycarbonyl protective group gave a fast rate, with a saturation in fluorescence reached after 24 h. The product formed is capable to cross the cell membrane, which is promising in view of prodrug activation in tissue: SCPNs would only have to be delivered locally, not intracellularly, to achieve the desired pro-drug to drug catalysis.

Our detailed study on the different factors affecting catalysis with SCPNs also revealed the challenges that need to be addressed to rationally design catalysts with potential for *in vivo* applications. Very high turnovers of the catalysts may compensate for this, but a better protection of the catalyst within the hydrophobic core of the particle could also help to increase the efficacy of the catalyst. For this reason, new SCPN-based catalysts with better shielding of the metal-complex and improved stability and activity are a necessary follow up of this work. Moreover, more selective substrates that maximize the interactions with the SCPNs versus other biological molecules have to be developed. Finally, the hydrolytic stability of the protective group has to be taken in account.

The development of catalytic systems that are able to perform their functions in living cells has been a subject of recent attention because of its potential applications in the fields of synthetic biology and therapeutic biomaterials. Notably, the use of artificial enzyme-like particles in the cellular environment is a frontier of the research in catalysis with potential applications in chemical biology and cancer therapy. However, the rational design of such structures is a huge chemical challenge, mostly due to the lack of knowledge on the behavior of catalytic systems in the complex biological environment and therefore on their structure−activity relations. Therefore, the biophysical study presented here, sheds light on the behavior of SCPNs in the cellular environment, paving the way toward the rational design of nanosystems that are able to perform effective catalysis *in vivo*.

ASSOCIATED CONTENT

Supporting Information

The Supporting Information is available free of charge on the ACS Publications website at DOI: 10.1021/jacs.8b00122.

Experimental and synthetic details, UV−vis spectra, CD spectra, ^{1}H NMR spectra, DLS, LC-MS traces (PDF)

AUTHOR INFORMATION

Corresponding Authors

*A. R. A. Palmans. E-mail: a.palmans@tue.nl.
*L. Albertazzi. E-mail: l.albertazzi@ibecbarcelona.eu.

ORCID

E. W. Meijer: 0000-0003-4126-7492
Lorenzo Albertazzi: 0000-0002-6837-0812
Anja R. A. Palmans: 0000-0002-7201-1548

Author Contributions

#Y. Liu and S. Pujals contributed equally to this work.

Notes

The authors declare no competing financial interest.

ACKNOWLEDGMENTS

Y.L., S.P., A.R.A.P. and E.W.M. acknowledge financial support from the Dutch Ministry of Education, Culture and Science (Gravity program 024.001.035) and the European Research Council (FP7/2007-2013, ERC Grant Agreement 246829). T.P. thanks the German Academic Exchange Service for financial support via a DAAD Research Fellowship for Postdoctoral Researchers. Dr. E. Huerta and Dr. M. Artar are acknowledged for fruitful discussions and Dr. B. de Waal for assistance with the MC-Rh 110 synthesis. The ICMS animation studio is acknowledged for providing the artwork. This work was financially supported by the AXA Research Fund (L.A.) and by the Spanish Ministry of Economy, Industry and Competitiveness through the Centro de Excelencia Severo Ochoa Award (L.A. and S.P.), by the Generalitat de Catalunya through the CERCA program. Moreover, this work was supported by the Spanish Ministry of Economy and Competitiveness through the project SAF2016-75241-R (MINECO/FEDER).

REFERENCES

(1) For reviews, see: (a) Ouchi, M.; Badi, N.; Lutz, J.-F.; Sawamoto, M. *Nat. Chem.* **2011**, *3*, 917−924. (b) Altintas, O.; Barner-Kowollik, C. *Macromol. Rapid Commun.* **2012**, *33*, 958−971. (c) Aiertza, M.; Odriozola, I.; Cabañero, G.; Grande, H.-J.; Loinaz, I. *Cell. Mol. Life Sci.* **2012**, *69*, 337−346. (d) Sanchez-Sanchez, A.; Perez-Baena, I.; Pomposo, J. A. *Molecules* **2013**, *18*, 3339−3355. (e) Sanchez-Sanchez, A.; Pomposo, J. A. *Part. Part. Syst. Char.* **2014**, *31*, 11−23. (f) Pomposo, J. A. *Polym. Int.* **2014**, *63*, 589−592. (g) Lyon, C. K.; Prasher, A.; Hanlon, A. M.; Tuten, B. T.; Tooley, C. A.; Frank, P. G.; Berda, E. B. *Polym. Chem.* **2015**, *6*, 181−197. (h) Gonzalez-Burgos, M.; Latorre-Sanchez, A.; Pomposo, J. A. *Chem. Soc. Rev.* **2015**, *44*, 6122−6142. (i) Altintas, O.; Barner-Kowollik, C. *Macromol. Rapid Commun.* **2016**, *37*, 29−46. (j) Hanlon, A. M.; Lyon, C. K.; Berda, E. B. *Macromolecules* **2016**, *49*, 2−14.

(2) (a) Mavila, S.; Eivgi, O.; Berkovich, I.; Lemcoff, N. G. *Chem. Rev.* **2016**, *116*, 878−961. (b) *Single-Chain Polymer Nanoparticles*: Synthesis, Synthesis, Characterization, Simulations and Applications; Pomposo, J. A., Ed.; Wiley-VCH: Weinheim, 2017.

DOI: 10.1021/jacs.8b00122
J. Am. Chem. Soc. 2018, 140, 3423−3433

(3) (a) Perez-Baena, I.; Asenjo-Sanz, I.; Arbe, A.; Moreno, A. J.; Lo Verso, F.; Colmenero, J.; Pomposo, J. A. *Macromolecules* **2014**, *47*, 8270−8280. (b) Hansell, C. F.; Lu, A.; Patterson, J. P.; O'Reilly, R. K. *Nanoscale* **2014**, *6*, 4102−4107. (c) Willenbacher, J.; Wuest, K. N. R.; Mueller, J. O.; Kaupp, M.; Wagenknecht, H.-A.; Barner-Kowollik, C. *ACS Macro Lett.* **2014**, *3*, 574−579. (d) Shishkan, O.; Zamfir, M.; Gauthier, M. A.; Borner, H. G.; Lutz, J.-F. *Chem. Commun.* **2014**, *50*, 1570−1572. (e) Sanchez-Sanchez, A.; Asenjo-Sanz, I.; Buruaga, L.; Pomposo, J. A. *Macromol. Rapid Commun.* **2012**, *33*, 1262−1267. (f) Frank, P. G.; Tuten, B. T.; Prasher, A.; Chao, D.; Berda, E. B. *Macromol. Rapid Commun.* **2014**, *35*, 249−253. (g) Sanchez-Sanchez, A.; Fulton, D. A.; Pomposo, J. A. *Chem. Commun.* **2014**, *50*, 1871−1874. (h) Whitaker, D. E.; Mahon, C. S.; Fulton, D. A. *Angew. Chem., Int. Ed.* **2013**, *52*, 956−959. (i) Tuten, B. T.; Chao, D.; Lyon, C. K.; Berda, E. B. *Polym. Chem.* **2012**, *3*, 3068−3071. (j) Murray, B. S.; Fulton, D. A. *Macromolecules* **2011**, *44*, 7242−7252. (k) Cole, J. P.; Lessard, J. J.; Lyon, C. K.; Tuten, B. T.; Berda, E. B. *Polym. Chem.* **2015**, *6*, 5555−5559. (l) Prasher, A.; Loynd, C. M.; Tuten, B. T.; Frank, P. G.; Chao, D. M.; Berda, E. B. *J. Polym. Sci., Part A: Polym. Chem.* **2016**, *54*, 209−217.

(4) (a) Ghosh, S.; Ramakrishnan, S. *Angew. Chem.* **2005**, *117*, 5577−5583. (b) Seo, M.; Beck, J. B.; Paulusse, J. M. J.; Hawker, C. J.; Kim, S. Y. *Macromolecules* **2008**, *41*, 6413−6418. (c) Foster, E. J.; Berda, E. B.; Meijer, E. W. *J. Am. Chem. Soc.* **2009**, *131*, 6964−6966. (d) Mes, T.; van der Weegen, R.; Palmans, A. R. A.; Meijer, E. W. *Angew. Chem., Int. Ed.* **2011**, *50*, 5085−5089. (e) Appel, E. A.; Barrio, J. D.; Dyson, J.; Isaacs, L.; Scherman, O. A. *Chem. Sci.* **2012**, *3*, 2278−2281. (f) Altintas, O.; Lejeune, E.; Gerstel, P.; Barner-Kowollik, C. *Polym. Chem.* **2012**, *3*, 640−651. (g) Gillissen, M. A. J.; Terashima, T.; Meijer, E. W.; Palmans, A. R. A.; Voets, I. K. *Macromolecules* **2013**, *46*, 4120−412. (h) Hosono, N.; Gillissen, M. A. J.; Li, Y. C.; Sheiko, S. S.; Palmans, A. R. A.; Meijer, E. W. *J. Am. Chem. Soc.* **2013**, *135*, 501−510. (i) Wang, F.; Pu, H.; Jin, M.; Pan, H. Y.; Chang, Z. H.; Wan, D. C.; Du, J. *J. Polym. Sci., Part A: Polym. Chem.* **2015**, *53*, 1832−1840.

(5) ter Huurne, G. M.; de Windt, L. N. J.; Liu, Y.; Meijer, E. W.; Voets, I. K.; Palmans, A. R. A. *Macromolecules* **2017**, *50*, 8562−8569.

(6) (a) Terashima, T.; Mes, T.; De Greef, T. F. A.; Gillissen, M. A. J.; Besenius, P.; Palmans, A. R. A.; Meijer, E. W. *J. Am. Chem. Soc.* **2011**, *133*, 4742−4745. (b) Huerta, E.; Stals, P. J. M.; Meijer, E. W.; Palmans, A. R. A. *Angew. Chem., Int. Ed.* **2013**, *52*, 2906−2910. (c) Sanchez-Sanchez, A.; Arbe, A.; Colmenero, J.; Pomposo, J. A. *ACS Macro Lett.* **2014**, *3*, 439−443. (d) Artar, M.; Souren, E. R. J.; Terashima, T.; Meijer, E. W.; Palmans, A. R. A. *ACS Macro Lett.* **2015**, *4*, 1099−1103. (e) Willenbacher, J.; Altintas, O.; Trouillet, V.; Knofel, N.; Monteiro, M. J.; Roesky, P. W.; Barner-Kowollik, C. *Polym. Chem.* **2015**, *6*, 4358−4365. (f) Liu, Y.; Pauloehrl, T.; Presolski, S. I.; Albertazzi, L.; Palmans, A. R. A.; Meijer, E. W. *J. Am. Chem. Soc.* **2015**, *137*, 13096−13105.

(7) (a) Bhowmik, D.; Pomposo, J. A.; Juranyi, F.; García-Sakai, V.; Zamponi, M.; Su, Y.; Arbe, A.; Colmenero, J. *Macromolecules* **2014**, *47*, 304−315. (b) Pomposo, J. A.; Ruiz de Luzuriaga, A.; Garcia, I.; Etxeberria, A.; Colmenero, J. *Macromol. Rapid Commun.* **2011**, *32*, 573−578.

(8) (a) Perez-Baena, I.; Loinaz, I.; Padro, D.; Garcia, I.; Grande, H. J.; Odriozola, I. *J. Mater. Chem.* **2010**, *20*, 6916−6922. (b) Benito, A. B.; Aiertza, M. K.; Marradi, M.; Gil-Iceta, L.; Shekhter Zahavi, T.; Szczupak, B.; Jiménez-González, M.; Reese, T.; Scanziani, E.; Passoni, L.; Matteoli, M.; De Maglie, M.; Orenstein, A.; Oron-Herman, M.; Kostenich, G.; Buzhansky, L.; Gazit, E.; Grande, H.-J.; Gómez-Vallejo, V.; Llop, J.; Loinaz, I. *Biomacromolecules* **2016**, *17*, 3213−3221.

(9) Gillissen, M. A. J.; Voets, I. K.; Meijer, E. W.; Palmans, A. R. A. *Polym. Chem.* **2012**, *3*, 3166−3174.

(10) Bai, Y.; Feng, X.; Xing, H.; Xu, Y.; Kim, B. K.; Baig, N.; Zhou, T.; Gewirth, A. A.; Lu, Y.; Oldfield, E.; Zimmerman, S. C. *J. Am. Chem. Soc.* **2016**, *138*, 11077−11080.

(11) (a) Prescher, J. A.; Bertozzi, C. R. *Nat. Chem. Biol.* **2005**, *1*, 13−21. (b) Sletten, E. M.; Bertozzi, C. R. *Angew. Chem., Int. Ed.* **2009**, *48*, 6974−6998. (c) Li, J.; Chen, P. R. *ChemBioChem* **2012**, *13*, 1728−1731. (d) Hartinger, C. G.; Metzler-Nolte, N.; Dyson, P. J. *Organometallics* **2012**, *31*, 5677−5685. (e) Sasmal, P. K.; Streu, K. N.; Meggers, E. *Chem. Commun.* **2013**, *49*, 1581−1587. (f) Yang, M.; Li, J.; Chen, P. R. *Chem. Soc. Rev.* **2014**, *43*, 6511−6526. (g) Li, Q.; van der Wijst, M. G. P.; Kazemier, H. G.; Rots, M. G.; Roelfes, G. *ACS Chem. Biol.* **2014**, *9*, 1044−1051. (h) Li, J.; Chen, P. R. *Nat. Chem. Biol.* **2016**, *12*, 129−137. (i) Jeschek, M.; Reuter, R.; Heinisch, T.; Trindler, C.; Klehr, J.; Panke, S.; Ward, T. R. *Nature* **2016**, *537*, 661−665.

(12) (a) Poizat, M.; Arends, I. W. C. E.; Hollmann, F. *J. Mol. Catal. B: Enzym.* **2010**, *63*, 149−156. (b) Wilson, Y. M.; Dürrenberger, M.; Nogueira, E. S.; Ward, T. R. *J. Am. Chem. Soc.* **2014**, *136*, 8928−8932.

(13) (a) Streu, C.; Meggers, E. *Angew. Chem., Int. Ed.* **2006**, *45*, 5645−5648. (b) Santra, M.; Ko, S.-K.; Shin, I.; Ahn, K. H. *Chem. Commun.* **2010**, *46*, 3964−3966. (c) Spicer, C. D.; Triemer, T.; Davis, B. G. *J. Am. Chem. Soc.* **2012**, *134*, 800−803. (d) Li, N.; Lim, R. K. V.; Edwardraja, S.; Lin, Q. *J. Am. Chem. Soc.* **2011**, *133*, 15316−15319. (e) Li, J.; Yu, J.; Zhao, J.; Wang, J.; Zheng, S.; Lin, S.; Chen, L.; Yang, M.; Jia, S.; Zhang, X.; Chen, P. R. *Nat. Chem.* **2014**, *6*, 352−361. (f) Sasmal, P. K.; Carregal-Romero, S.; Parak, W. J.; Meggers, E. *Organometallics* **2012**, *31*, 5968−5970. (g) Bevilacqua, V.; King, M.; Chaumontet, M.; Nothisen, M.; Gabillet, S.; Buisson, D.; Puente, C.; Wagner, A.; Taran, F. *Angew. Chem., Int. Ed.* **2014**, *53*, 5872−5876. (h) Sánchez, M. I.; Penas, C.; Eugenio Vázquez, M.; Mascareñas, J. L. *Chem. Sci.* **2014**, *5*, 1901−1907. (i) Tomás-Gamasa, M.; Martínez-Calvo, M.; Couceiro, J. R.; Mascareñas, J. L. *Nat. Commun.* **2016**, *7*, 12538. (j) Bose, S.; Ngo, A. H.; Do, L. H. *J. Am. Chem. Soc.* **2017**, *139*, 8792−8795. (k) Völker, T.; Meggers, E. *ChemBioChem* **2017**, *18*, 1083−1086. (l) Indrigo, E.; Clavadetscher, J.; Chankeshwara, S. V.; Megia-Fernandez, A.; Lilienkampf, A.; Bradley, M. *Chem. Commun.* **2017**, *53*, 6712−6715.

(14) (a) Thielbeer, F.; Chankeshwara, S. V.; Johansson, E. M. V.; Norouzi, N.; Bradley, M. *Chem. Sci.* **2013**, *4*, 425−431. (b) Unciti-Broceta, A.; Johansson, E. M. V.; Yusop, R. M.; Sanchez-Martin, M.; Bradley, M. *Nat. Protoc.* **2012**, *7*, 1207−1218. (c) Yusop, R. M.; Unciti-Broceta, A.; Johansson, E. M. V.; Sanchez-Martin, R. M.; Bradley, M. *Nat. Chem.* **2011**, *3*, 239−243. (d) Wang, J.; Cheng, B.; Li, J.; Zhang, Z.; Hong, W.; Chen, X.; Chen, P. R. *Angew. Chem., Int. Ed.* **2015**, *54*, 5364−5368. (e) Tonga, G. Y.; Jeong, Y.; Duncan, B.; Mizuhara, T.; Mout, R.; Das, R.; Kim, S. T.; Yeh, Y.-C.; Yan, B.; Hou, S.; Rotello, V. M. *Nat. Chem.* **2015**, *7*, 597−603. (f) Perez-Lopez, A. M.; Rubio-Ruiz, B.; Sebastian, V.; Hamilton, L.; Adam, C.; Bray, T. L.; Irusta, S.; Brennan, P. M.; Lloyd-Jones, G. C.; Sieger, D.; Santamaria, J.; Unciti-Broceta, A. *Angew. Chem., Int. Ed.* **2017**, *56*, 12548−12552.

(15) (a) Weiss, J. T.; Dawson, J. C.; Macleod, K. G.; Rybski, W.; Fraser, C.; Torres-Sanchez, C.; Patton, E. E.; Bradley, M.; Carragher, N. O.; Unciti-Broceta, A. *Nat. Commun.* **2014**, *5*, 3277. (b) Weiss, J. T.; Dawson, J. C.; Fraser, C.; Rybski, W.; Torres-Sanchez, C.; Bradley, M.; Patton, E. E.; Carragher, N. O.; Unciti-Broceta, A. *J. Med. Chem.* **2014**, *57*, 5395−5404. (c) Weiss, J. T.; Carragher, N. O.; Unciti-Broceta, A. *Sci. Rep.* **2015**, *5*, 9329. (d) Rubio-Ruiz, B.; Weiss, J. T.; Unciti-Broceta, A. *J. Med. Chem.* **2016**, *59*, 9974−9980. (e) Indrigo, E.; Clavadetscher, J.; Chankeshwara, S. V.; Lilienkampf, A.; Bradley, M. *Chem. Commun.* **2016**, *52*, 14212−14214. (f) Clavadetscher, J.; Hoffmann, S.; Lilienkampf, A.; Mackay, L.; Yusop, R. M.; Rider, S. A.; Mullins, J. J.; Bradley, M. *Angew. Chem., Int. Ed.* **2016**, *55*, 15662−15666. (g) Clavadetscher, J.; Indrigo, E.; Chankeshwara, S. V.; Lilienkampf, A.; Bradley, M. *Angew. Chem., Int. Ed.* **2017**, *56*, 6864−6868. (h) Miller, M. A.; Askevold, B.; Mikula, H.; Kohler, R. H.; Pirovich, D.; Weissleder, R. *Nat. Commun.* **2017**, *8*, 15906.

(16) (a) Dougherty, T. J.; Grindey, G. B.; Fiel, R.; Weishaupt, K. R.; Boyle, D. G. *J. Natl. Cancer Inst.* **1975**, *55*, 115−121. (b) DeRosa, M. C.; Crutchley, R. J. *Coord. Chem. Rev.* **2002**, *233/234*, 351−371. (c) Allison, R. R.; Downie, G. H.; Cuenca, R.; Hu, X.-H.; Childs, C. J. H.; Sibata, C. H. *Photodiagn. Photodyn. Ther.* **2004**, *1*, 27−42. (d) Dolmans, D. E. J. G. J.; Fukumura, D.; Jain, R. K. *Nat. Rev. Cancer* **2003**, *3*, 380−387. (e) Agostinis, P.; Berg, K.; Cengel, K. A.; Foster, T. H.; Girotti, A. W.; Gollnick, S. O.; Hahn, S. M.; Hamblin, M. R.; Juzeniene, A.; Kessel, D.; Korbelik, M.; Moan, J.; Mroz, P.; Nowis, D.;

DOI: 10.1021/jacs.8b00122
J. Am. Chem. Soc. 2018, 140, 3423−3433

Piette, J.; Wilson, B. C.; Golab, J. *Ca-Cancer J. Clin.* **2011**, *61*, 250−281.
(17) Presolski, S. I.; van der Weegen, R.; Wiesfeld, J. J.; Meijer, E. W. *Org. Lett.* **2014**, *16*, 1864−1867.
(18) (a) Lewis, W. G.; Magallon, F. G.; Fokin, V. V.; Finn, M. G. *J. Am. Chem. Soc.* **2004**, *126*, 9152−9153. (b) Yang, M.; Jalloh, A. S.; Wei, W.; Zhao, J.; Wu, P.; Chen, P. R. *Nat. Commun.* **2014**, *5*, 4981.
(19) (a) Engle, K. M.; Yu, J.-Q. *J. Org. Chem.* **2013**, *78*, 8927−8955. (b) Campbell, A. N.; White, P. B.; Guzei, I. A.; Stahl, S. S. *J. Am. Chem. Soc.* **2010**, *132*, 15116−15119.
(20) (a) Bojinov, V. B.; Georgiev, N. I.; Nikolov, P. S. *J. Photochem. Photobiol., A* **2008**, *193*, 129−138. (b) Bardajee, G. R.; Li, A. Y.; Haley, J. C.; Winnik, M. A. *Dyes Pigm.* **2008**, *79*, 24−32.
(21) Elsabahy, M.; Wooley, K. L. *Chem. Soc. Rev.* **2012**, *41*, 2545−2561.
(22) (a) Albertazzi, L.; Fernandez-Villamarin, M.; Riguera, R.; Fernandez-Megia, E. *Bioconjugate Chem.* **2012**, *23*, 1059−1068. (b) Albertazzi, L.; Storti, B.; Marchetti, L.; Beltram, F. *J. Am. Chem. Soc.* **2010**, *132*, 18158−18167. (c) Bazban-Shotorbani, S.; Hasani-Sadrabadi, M. M.; Karkhaneh, A.; Serpooshan, V.; Jacob, K. I.; Moshaverinia, A.; Mahmoudi, M. *J. Controlled Release* **2017**, *253*, 46−63.
(23) Potter, H.; Heller, R. *Curr. Protoc. Mol. Biol.* **2010**, *92*, 9.3.1−9.3.10.
(24) Atanasova, S.; Nikolova, B.; Murayama, S.; Stoyanova, E.; Tsoneva, I.; Zhelev, Z.; Aoki, I.; Bakalova, R. *Anticancer Res.* **2016**, *36*, 4601−4606.
(25) (a) Bizzarri, R.; Cardarelli, F.; Serresi, M.; Beltram, F. *Anal. Bioanal. Chem.* **2012**, *403*, 2339−2351. (b) Samudram, A.; Mangalassery, B. M.; Kowshik, M.; Patincharath, N.; Varier, G. K. *Cell Biol. Int.* **2016**, *40*, 991−998.
(26) (a) Ramsey, J. D.; Flynn, N. H. *Pharmacol. Ther.* **2015**, *154*, 78−86. (b) Florén, A., Mäger, I., Langel, Ü. Uptake Kinetics of Cell-Penetrating Peptides. In *Cell-penetrating peptides: methods and protocols*; Langel, Ü., Ed.; Humana Press: Totowa, 2011. (c) Kataoka, K.; Kwon, G. S.; Yokoyama, M.; Okano, T.; Sakurai, Y. *Pharm. Res.* **1993**, *24*, 119−132. (d) Otsuka, H.; Nagasaki, Y.; Kataoka, K. *Adv. Drug Delivery Rev.* **2003**, *55*, 403−419.
(27) Adler, M.; Shafer, H.; Hamilton, T.; Petrali, J. P. *Neurotoxicology* **1999**, *20*, 571−582.
(28) (a) Nishiyama, N.; Morimoto, Y.; Jang, W. D.; Kataoka, K. *Adv. Drug Delivery Rev.* **2009**, *61*, 327−338. (b) Jeong, Y.-H.; Yoon, H.-J.; Jang, W.-D. *Polym. J.* **2012**, *44*, 512−521. (c) Gibot, L.; Lemelle, A.; Till, U.; Moukarzel, B.; Mingotaud, A.-F.; Pimienta, V.; Saint-Aguet, P.; Rols, M.-P.; Gaucher, M.; Violleau, F.; Chassenieux, C.; Vicendo, P. *Biomacromolecules* **2014**, *15*, 1443−1455. (d) Rajora, M. A.; Lou, J. W. H.; Zheng, G. *Chem. Soc. Rev.* **2017**, *46*, 6433−6469.
(29) (a) Liu, W.; Chen, C.; Tang, X.; Shi, J.; Zhang, P.; Zhang, K.; Li, Z.; Dou, W.; Yang, L.; Liu, W.; et al. *Inorg. Chem.* **2014**, *53*, 12590−12594. (b) Chen, Y.; Zhang, M.; Han, Y.; Wei, J. *RSC Adv.* **2016**, *6*, 8380−8383.
(30) (a) Lavis, L. D.; Chao, T.-Y.; Raines, R. T. *ACS Chem. Biol.* **2006**, *1*, 252−260. (b) Terentyeva, T. G.; Van Rossom, W.; Van der Auweraer, M.; Blank, K.; Hofkens, J. *Bioconjugate Chem.* **2011**, *22*, 1932−1938. (c) Wang, Z.-Q.; Liao, J.; Diwu, Z. *Bioorg. Med. Chem. Lett.* **2005**, *15*, 2335−2338.
(31) (a) Bertrand, P.; Gesson, J. P. *J. Org. Chem.* **2007**, *72*, 3596−3599. (b) Kislukhin, A. A.; Hong, V. P.; Breitenkamp, K. E.; Finn, M. G. *Bioconjugate Chem.* **2013**, *24*, 684−689.
(32) Liu, Y.; Turunen, P.; Blank, K.; Rowan, A. E.; Palmans, A. R. A.; Meijer, E. W. Manuscript in preparation.

DOI: 10.1021/jacs.8b00122
J. Am. Chem. Soc. 2018, 140, 3423−3433